Optica Applicata, Vol. XLI, No. 3, 2011

Significant effect of oxygen atmosphere on the structure, optical and electrical properties of Ti-doped In_2O_3 transparent conductive thin films

C.J. DONG[1, 2, 3], W.X. YU[1], M. XU[3], C. CHEN[2], Z.Y. SONG[2], L. LI[2], Y.D. WANG[2*]

[1]Department of Materials Science, Jilin University, Changchun 130012, P.R. China

[2]State Key Laboratory on Integrated Optoelectronics, College of Electronic Science and Engineering, Jilin University, Changchun 130012, P.R. China

[3]Lab for Low-dimensional Structure Physics, Institute of Solid State Physics, Sichuan Normal University, Chengdu 610068, P.R. China

[*]Corresponding author: wangyiding47@yahoo.com.cn

Titanium-doped indium oxide (In_2O_3) transparent conductive thin films were deposited on glass and sapphire (0001) substrates with/without oxygen atmosphere by DC magnetron sputtering at 300 °C. The content of titanium is estimated to be about 1.8 at.% using energy dispersive spectroscopy. The smooth surfaces were covered with more uniform octahedral grains. X-ray diffraction measurements indicated that the preferential growth orientation along the (400) plane for the sample grown without oxygen atmosphere shifts to (222) for the sample grown in the oxygen atmosphere. The average optical transmittance of the sample grown with the introduction of oxygen varies from 70% to 90% in the visible region, which corresponds well to the variation of carrier and mobility. Hence, both intermediate dopant and oxygen atmosphere will provide the optimum balance between carrier concentration and mobility leading to the best transport properties of Ti-doped In_2O_3 films.

Keywords: transparent oxide, indium oxide, thin films, electrical properties, optical properties.

1. Introduction

Transparent conductive oxide (TCO) material is an interesting semiconductor owing to its unique properties of both high electrical conductivity and high optical transparency [1, 2]. As a matrix for the generation of transparent conducting oxides, indium oxide (In_2O_3) has been the subject of numerous studies for liquid crystal displays [3], solar cell [4], sensors [5], nanowire technology [6], light emitting diodes, and other optoelectronic devices. Recently, it has been reported that the origin of the native donor in undoped In_2O_3 is interstitial indium, but also that the existence of an oxygen vacancy

is absolutely essential for carrier generation [7]. Due to the presence of intrinsic oxygen vacancies in the lattice [8], In_2O_3 is of transparent wide bandgap [9] and *n*-type conductivity. In order to increase the transparency without compromising the conductivity, the carrier concentration needs to be decreased while the mobility is increased. A promising approach to overcome this limit is the growth of high quality In_2O_3 with extrinsic *n*-type dopants, such as Sn [10, 11], Ti [12, 13], Mo [1, 14], W [15] and so on, which has been widely investigated by means of experiments and calculation based on the density functional theory (DFT) [8, 16].

Indium tin oxide (ITO) in commercial grade fabricated on glass has σ = = 5000 $S\,cm^{-1}$, μ = 47 $cm^2V^{-1}s^{-1}$ and $n = 6.6\times10^{20}$ cm^{-3} [10], however, in research grade ITO films grown on yttria-stabilized zirconia (YSZ) by pulsed laser deposition it possesses σ = 13000 $S\,cm^{-1}$, μ = 42 $cm^2V^{-1}s^{-1}$ and $n = 1.9\times10^{21}$ cm^{-3} (optical transmission exceeding 85% at wavelengths from 340 to 780 nm) [11]. Currently, it is shown that using molybdenum instead of tin produces an IMO material with very high carrier mobility. Mo-doped indium oxide (IMO) thin films deposited on glass substrates by a spray pyrolysis experimental technique has σ = 1886 $S\,cm^{-1}$ with μ = 122.4 $cm^2V^{-1}s^{-1}$ and $n = 9.5\times10^{19}$ cm^{-3} (average transparency of 83% in the wavelengths ranging from 400 to 2500 nm) [1] and IMO films with σ = 5900 $S\,cm^{-1}$, μ > 100 $cm^2V^{-1}s^{-1}$ and $n = 3\times10^{20}$ cm^{-3} (transparency greater than 80%) have also been reported [14]. The highest mobility was observed at a W-dopant concentration of 0.03 with σ = 3100 $S\,cm^{-1}$, μ = 66 $cm^2V^{-1}s^{-1}$ and $n = 2.90\times10^{20}$ cm^{-3} (high visible transmittance of 80%) [15]. Titanium is another important dopant for indium oxide with good conductivity and high mobility material. Ti-doped indium oxide with σ = 6260 $S\,cm^{-1}$, μ = 83.3 $cm^2V^{-1}s^{-1}$ and $n = 8.0\times10^{20}$ cm^{-3} (transparency greater than 85% at wavelengths from 400 to 1750 nm) [12] and highest mobility μ = 159 $cm^2V^{-1}s^{-1}$ with σ = 10858 $S\,cm^{-1}$ and $n = 4.3\times10^{20}$ cm^{-3} (transparency of 83%) [13] has been reported. However, all of the Ti-doped indium oxide samples were grown under either pure argon [12] or oxygen ambient [13]. Since the In_2O_3 cubic bixbyite structure with a lattice parameter of 10.117 Å has proven to be related with the ordered oxygen vacancy [17], the vacancy oxygen is believed to play important roles in achieving the transparent and conducting properties of In_2O_3. As is known, indium oxide films grown in pure argon ambient have a dark appearance and poor optical properties due to the lack of oxygen [18]. However, the co-sputtered titanium doped indium oxide films in Ar-only ambient do have good optical properties and do not show this darkening [1]. The effect of oxygen pressure during growth on the optical transparency of Mo-doped In_2O_3 films has been studied [14, 19], but it is still unclear how the growth conditions with or without oxygen atmosphere affect the crystalline structure, electrical, optical properties and surface morphology of Ti-doped In_2O_3 films. This scarcity calls for in-depth experimental analysis.

In this paper, we successfully synthesized polycrystalline Ti-doped In_2O_3 films on glass and sapphire (0001) substrates with or without oxygen atmosphere. The effect of oxygen atmosphere on the properties such as crystalline structure, surface morphology and optical and electrical properties of Ti-doped In_2O_3 films was

discussed. Our results are very helpful in optimizing the growth of Ti-doped In_2O_3 TCO films.

2. Experiment

Ti-doped In_2O_3 films were fabricated on glass and sapphire (0001) substrates by DC magnetron sputtering with a power of 50 W using an oxide ceramic In_2O_3-TiO_2 target (98 wt% In_2O_3 and 2 wt% TiO_2) at temperature of 300 °C. A series of preliminary experiments have been done to optimize the growth conditions. Before being loaded into the sputtering chamber, the substrates were ultrasonically cleaned with acetone, rinsed with both ethanol and deionized water, and subsequently blow-dried with nitrogen gas. The vacuum chamber was initially evacuated to a base pressure of 5×10^{-5} Pa by a turbomolecular pumping system. Thereafter, Ti-doped In_2O_3 films were grown under pure 100% Ar flow of 10 sccm (sccm denotes cubic centimeter per minute at standard temperature and pressure (STP)) and mixture of argon-oxygen atmosphere with oxygen of 2 sccm at a fixed pressure of 1 Pa on glass and sapphire. These samples deposited on glass without and with oxygen atmosphere have been correspondingly marked as S_1 and S_2, respectively. S_3 and S_4 represent the samples deposited on sapphire in the conditions without and with oxygen atmosphere. To alleviate contamination, the target was cleaned by pre-sputtering for 20 min prior to the film growth and high purity Ar (99.999%) and O_2 (99.999%) were introduced through separate mass flow controllers.

The deposited Ti-doped In_2O_3 films were characterized and analyzed by scanning electron microscopy (SEM) (JEOL JEM-6700F at 3.0 kV), X-ray diffraction (XRD) (Rigaku D/max-2500 X-ray diffractometer system with Cu Kα radiation of 1.5418 Å), optical transmission measurements (UV-1700, SHIMADZU), and energy dispersive spectroscopy (EDS). To characterize the electrical properties, the Hall effect measurements were also carried out in the Van der Pauw configuration with indium ohmic electrodes by Bio-Rad Microscience HL5500 Hall System at room temperature.

3. Results and discussion

Figure 1 shows the SEM images of Ti-doped In_2O_3 thin films deposited without and with oxygen flow on glass and sapphire substrates. It is seen that the surface is smooth and well covered with uniformly distributed grains and is free from any pinholes or islands. Viewed from the top angle, the shape of grains is of octahedron. In general, the grain sizes are approximately estimated by the distance between the visible grain boundaries. One can see that the films prepared without oxygen flow on glass and sapphire exhibit an inhomogeneous size distribution from a few nanometers to about ~100 nm, *i.e.*, some areas include larger grains whereas some have smaller grains. The grain sizes become bigger and more uniform for the sample on sapphire under the growth conditions with oxygen atmosphere. For the samples on glass, the average grain size even exhibits opposite tendency after the participation of oxygen.

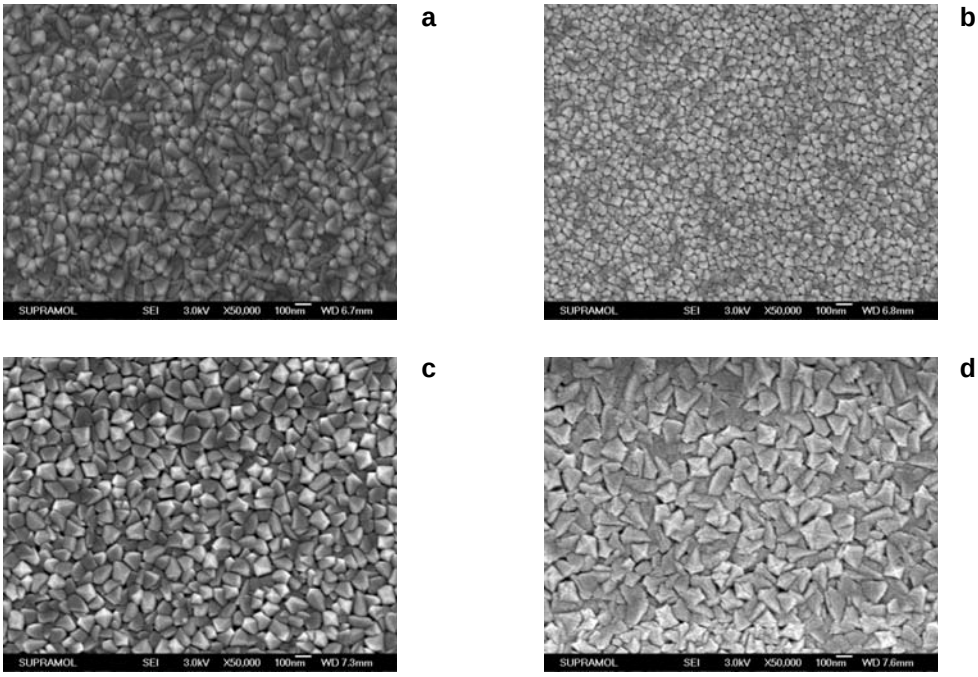

Fig. 1. SEM micrograph of Ti-doped In_2O_3 thin films prepared without and with oxygen atmosphere on glass and sapphire, denoted as S_1 (**a**), S_2 (**b**), S_3 (**c**), and S_4 (**d**).

Significantly, grain size for films deposited on glass is smaller than that on sapphire regardless of the oxygen atmosphere. On the other hand, the difference in morphology corresponds well to the different growth orientation, as is evidenced by the XRD measurements in the following.

Figure 2 displays the cross-section SEM view of Ti-doped In_2O_3 thin films grown without and with oxygen atmosphere on sapphire substrates (sample S_3 and S_4). It can be seen that the Ti-doped In_2O_3 films are continuous to stand on the sapphire substrate and consist of compacted pillar crystals with an average uniform height of ~500 nm.

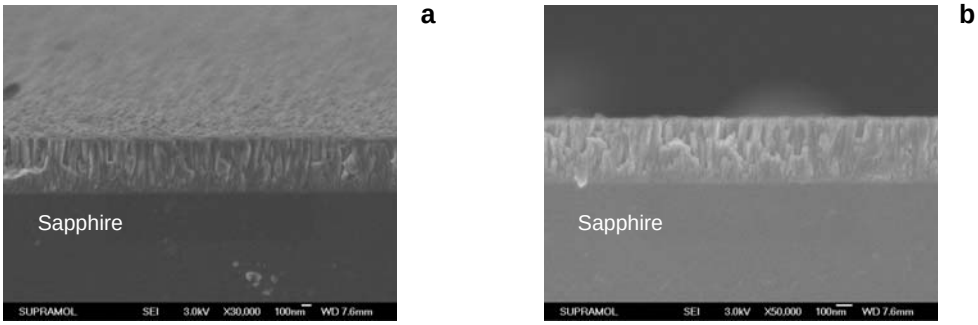

Fig. 2. SEM images showing a cross-section of sample S_3 (**a**), and S_4 (**b**).

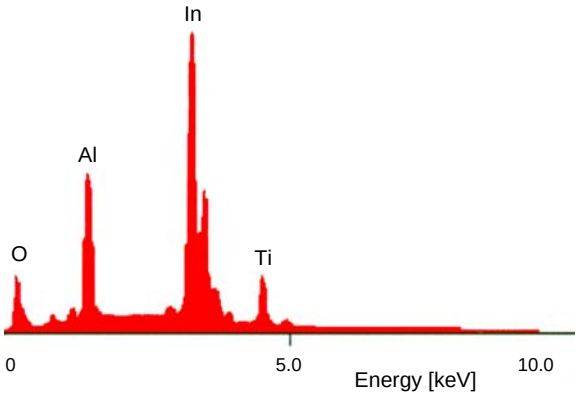

Fig. 3. Typical EDS results for sample S_4 (prepared with oxygen atmosphere on sapphire).

No apparent distinctive shape is observed between Ti-doped In_2O_3 thin films grown without or with oxygen atmosphere.

To determine the actual composition of the constituents, the films were further analyzed by using energy dispersion spectroscopy (EDS). A typical EDS spectrum (sample S_4), as shown in Fig. 3, indicates that the Ti-doped In_2O_3 films deposited on sapphire substrate with oxygen flow are composed of In, O, Ti and Al. Apparently, the aluminium peak comes from the sapphire substrate. The constituent of titanium is estimated to be ~1.8 at.%, corresponding to the Ti concentrations of 1.5–2.5 at.% for the Ti-doped In_2O_3 with the mobility maximum [12].

The XRD patterns of the Ti-doped In_2O_3 films deposited on the glass and sapphire substrate are given in Fig. 4**b**. For the purpose of comparison, a pure In_2O_3 bulk

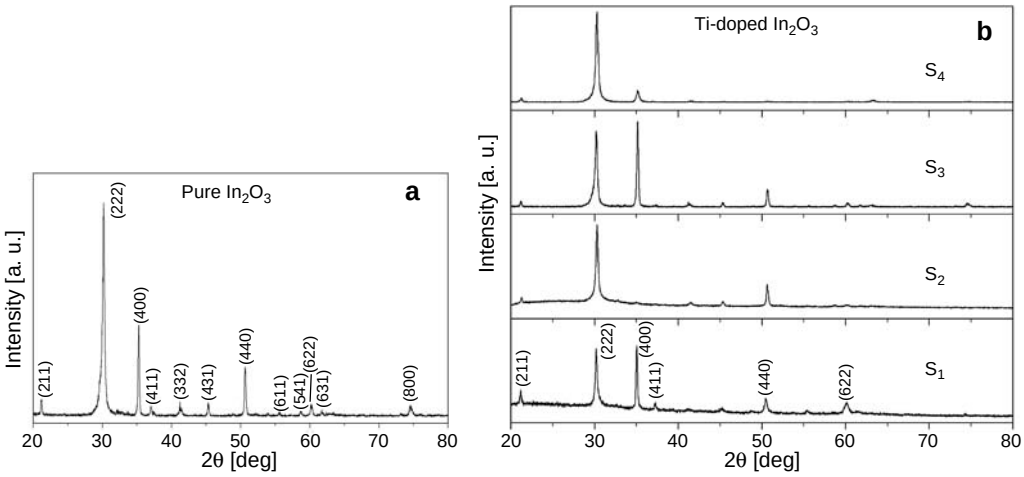

Fig. 4. XRD patterns of the typical pure In_2O_3 film deposited on the sapphire (**a**) and Ti-doped In_2O_3 films deposited on the glass and sapphire substrates without and with oxygen atmosphere denoted as S_1, S_2, S_3, and S_4, respectively (**b**).

X-ray experiment has been performed and shown in Fig. 4**a**. The diffraction peaks are identified and indexed according to the data of cubic In_2O_3 (JCPDS: 06-0416) [20] with lattice parameter of a = 10.1178 Å, which is in good agreement with the standard value of a = 10.12 Å. All of the diffraction peaks of the Ti-doped In_2O_3 are identified as the cubic In_2O_3 by matching with the pure bulk In_2O_3 film and standard data. No peaks corresponding to Ti or TiO_2 are observed although Ti amount is confirmed by EDS analysis. However, it is perceptible from Fig. 4**b** that the (222) and (400) peaks are different under different oxygen atmosphere. Clearly, the (222) diffraction intensity of the sample without the participation of oxygen is slightly stronger than that of the (400) diffraction peak as displayed as sample S_1 and S_3. With oxygen flow, the (222) diffraction intensity of the sample is apparently stronger than that of the (400) diffraction peak shown by S_2 and S_4. The data subtracted from the XRD data are listed in Tab. 1 for comparison purposes. There is no obvious XRD peak position shift for our Ti-doped samples compared with pure bulk In_2O_3 film. The value of full width at half maximum (FWHM) obtained from the (222) and (400) diffraction peaks of Ti-doped In_2O_3 varied from 0.080° to 0.350° with different oxygen atmosphere and substrates. The average particle size D of the thin films was evaluated using the Scherrer equation [21]:

$$D = \frac{k\lambda}{\beta \cos\theta} \tag{1}$$

where D is the crystal size in nm, and k is a constant with a value about 0.9 for Cu target, λ (1.5418 Å), β, and θ are the source wavelength, peak FWHM and peak position, respectively. It is evident that the grain size increased with introduction of oxygen flow. However, the grain sizes estimated from the XRD data are smaller than the values gained from SEM microstructure. Similar results have also been observed for Mo doped In_2O_3 [22], where the grain size obtained from the scanning electron

T a b l e 1. Data extracted from the XRD analysis.

Substrate	Sample	Angle 2θ [deg]	*hkl*	Lattice constant a [Å]	I_{222}/I_{400}	FWHM [deg]	Crystallite size [nm]
Glass	S_1	30.176	(222)	10.1228	0.80	0.240	27.6
		35.027	(400)	10.1242		0.160	67.0
	S_2	30.287	(222)	10.1221	43.48	0.313	37.8
		35.006	(400)	10.1124		0.080	100.0
Sapphire (Al_2O_3)	S_3	30.179	(222)	10.1201	0.82	0.350	24.6
		35.120	(400)	10.1024		0.194	50.1
	S_4	30.300	(222)	10.1210	12.35	0.319	27.2
		35.240	(400)	10.1078		0.191	51.2
Pure In_2O_3		30.110	(222)	10.1178	2.34	0.321	25.6
		35.217	(400)	10.1056		0.219	50.4

microscopy (SEM) microstructures was larger since smaller crystallites were agglomerated together to form larger grains.

The intensity ratio I_{222}/I_{400} given in Tab. 1 is used to evaluate the texture of the Ti-doped In_2O_3 films. The ratio value of about 0.8 is obtained for the Ti-doped In_2O_3 films deposited without oxygen flow, which is much smaller than 2.34 for pure films, while far larger values than the value of pure In_2O_3 films for the films prepared with oxygen flow are investigated. This indicates a strong crystallographic texture along the [100] direction for Ti-doped In_2O_3 films deposited without oxygen flow, however, the strong crystallographic texture changes along the [111] direction with participation of oxygen in the growth atmosphere. It is worthwhile to note that the lattice constants determined from XRD patterns ranged from 10.1024 to 10.1242 Å (Tab. 1), which are rather close to the data of pure In_2O_3 (10.1178 Å). This can be attributed to the fact that titanium ions are lightly smaller than indium ions [23] and the lower titanium amount was confirmed by EDS analysis. Similar phenomena were observed in the reports of Mo doped In_2O_3 [24] and other results of titanium doped In_2O_3 [12]. Due to the existence of titanium in our samples, this is further evidence that doped titanium atoms in the In_2O_3 do not significantly affect the lattice constant.

In_2O_3 is in the ordered vacancy structure [17] with 8 formula units, here 4 In atoms out of 16 occupy the centers of the trigonally distorted octahedral denoted as In(1) position (Wycoff 8*b* positions), while the rest are located at the centers of the tetragonally distorted octahedral figured as In(2) (Wycoff 24*d* positions). Thus, two substitutional disorders in In sublattices may appear when Ti substitutes in the In(1) and In(2) sublattices, respectively. Similar behavior has been investigated upon doping with Sn [24] and Mo [25] using first principles. On the other hand, the interstitial oxygen has significant impact on the properties of mobility and the free carrier concentration, which further makes complexes for Ti-doped In_2O_3 films. Apart from four kinds of intrinsic point defects (O vacancy, In interstitial, O interstitial, and In vacancy) [26], using Kröger–Vink notation, the following complicated defects were presumedly considered: $Ti^{\bullet}_{In(1)}$, $Ti^{\bullet}_{In(2)}$, $[Ti^{\bullet}_{In(1)} + 2In_{In}O_i'']'$, and $[Ti^{\bullet}_{In}\,O_i']'$, where the subscript stands for lattice site that the species occupies and superscript corresponds to the electronic charge of the species relative to the site that it occupies. Clearly, a good agreement with the other reported can be found, with one carrier per one Ti atom due to Ti^{4+} substituting for one In^{3+} [12]. In the oxygen atmosphere, facilitating the formation of $[Ti^{\bullet}_{In(1)} + 2In_{In}O_i'']'$, and $[Ti^{\bullet}_{In}\,O_i']'$ complexes, markedly reduces the number of free carriers but the mobility is improved owing to compensation effect of oxygen and the longer relaxation times, as is proved by the following Hall effect measurements. Unlike the Sn-doped case (with spherically symmetric *s* states) [27], as a transition metal, Ti *d* states are more sensitive to the surrounding oxygen. Therefore, theoretic analysis will be very helpful to look further into the Ti-doped case.

Figure 5 displays the transmittance of Ti-doped In_2O_3 films on the glass and sapphire substrates without and with oxygen atmosphere, respectively. Obviously, the average optical transmittance in the visible region fluctuates with the oxygen

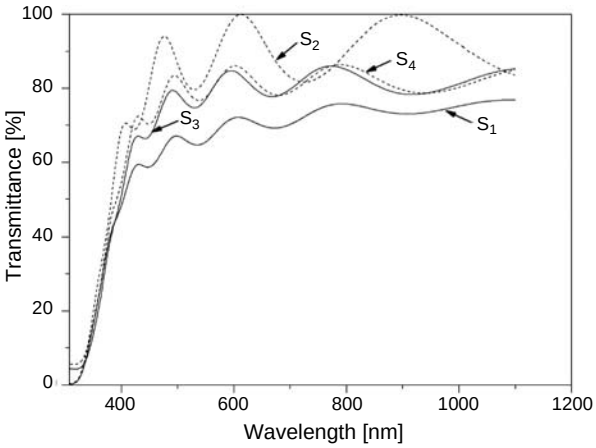

Fig. 5. Optical transmittance spectra of Ti-doped In_2O_3 films deposited on the glass and sapphire substrates without and with oxygen atmosphere, in visible range.

atmosphere and substrates. The higher transmittance in excess of 90% is obtained by Ti-doped In_2O_3 films deposited on the glass with oxygen atmosphere (denoted as S_2) corresponding to 70% for the sample grown without oxygen (denoted as S_1). However, the average optical transmittance of 85% is achieved regardless of oxygen atmosphere (denoted as S_3 and S_4) for Ti-doped In_2O_3 films deposited on the sapphire substrate. Usually, films grown under oxygen atmosphere are more transparent compared with the films grown under only argon or vacuum keeping other grown parameters.

The change of optical transmittance is mainly due to the influence of carrier and mobility shown in Tab. 2 by Hall effect measurements. After introduction of oxygen flow, the carrier concentrations of the films decrease, whereas the electron mobility is improved. The highest electron concentration can be obtained in samples grown in pure 100% Ar environment, however, the unintentional presence of oxygen impurities is almost unavoidable for samples deposition. From Table 2, one can see that the carrier concentration exhibits a steep decrease from 2.48×10^{20} cm^{-3} to 8.82×10^{18} cm^{-3} as oxygen is introduced in the growth of the films on glass, which is attributed to compensation by oxygen atoms. The film deposited on sapphire shows a decrease of carrier concentration from 8.83×10^{19} cm^{-3} to 2.17×10^{19} cm^{-3} with the introduction of oxygen. The carrier concentration for sample S_2 is even lower than an undoped In_2O_3 single crystal with carrier concentration of approximately 1×10^{19} cm^{-3}, as reported by KANAI [28]. Thus, by varying the dopants and amount of oxygen, one can concurrently control both the mobility and the carrier concentration. The amplified

T a b l e 2. Electrical properties of Ti-doped In_2O_3 films.

Samples	S_1	S_2	S_3	S_4
Electron mobility [cm^{2}V^{-1}s^{-1}]	3.59	27.5	4.56	6.97
Carrier concentrations [cm^{-3}]	2.48×10^{20}	8.82×10^{18}	8.83×10^{19}	2.17×10^{19}

scope change of electron mobility and carrier concentrations could be the reason for variation of transmittance between S_1 and S_2. This can be understood as follows: increasing the carrier concentration is the preferred route to optimizing the electrical conductivity, thereby resulting in transparency losses from carrier absorption. Thus, both intermediate dopant and oxygen atmosphere will provide the optimum balance between carrier concentration and mobility leading to the best transport properties of Ti-doped In_2O_3 films. In the case of titanium doping, one carrier per one Ti atom due to Ti^{4+} substituting for one In^{3+} [12] and for W doping as many as three carriers per W due to W^{6+} substitution on In^{3+} have been reported [15]. For Mo doping, one carrier per four Mo atoms [10] and for Sn doping at best one carrier per two Sn atoms have been investigated [29]. A sharp UV-off is observed to shift to the shorter wavelength with the increase of carrier concentration because the occupation of the dispersive conduction band with electrons induces a shift and widening of the energy gap, a process widely referred to as the Burstein–Moss (BM) shift [24]. It is believed that the high concentration of the extra carriers introduced by the dopant provides a pronounced BM shift, which was discussed in the case of tin-doped In_2O_3 system [27].

4. Conclusions

In summary, Ti-doped In_2O_3 films were grown with or without oxygen flow on glass and sapphire substrates by DC magnetron sputtering at 300 °C. The lower titanium concentration of 1.8 at.% in film has been evaluated. The XRD measurements indicate that the Ti-doped In_2O_3 films are polycrystalline films with a cubic bixbyite structure, but there is a change of preferred growth orientation after participation of oxygen atmosphere, as evidenced in the change of shape of surface morphology. The grains are of octahedral shape and grow larger as the oxygen flow is used. An increase of electron mobility but a decrease in carrier concentrations after participation of oxygen atmosphere is observed. The effect of oxygen atmosphere on the average transmittance for films deposited on glass is more significant than for the films grown on sapphire. Our results are highly relevant to the optimization growth of transparent conductive thin films.

Acknowledgements – This work was financially supported by the National High-Technology Research and Development Program (“863” Program) of China (Grant Nos. 2007AA03Z446, 2007AA06Z112 and 2009AA03Z442), the Science and Technology Department of Jilin Province (Nos. 20070709 and 20090422).

References

[1] PARTHIBAN S., ELANGOVAN E., RAMAMURTHI K., MARTINS R., FORTUNATO E., *High near-infrared transparency and carrier mobility of Mo doped In_2O_3 thin films for optoelectronics applications*, Journal of Applied Physics **106**(6), 2009, p. 063716.

[2] KOIDA T., KONDO M., *High-mobility transparent conductive Zr-doped In_2O_3*, Applied Physics Letters **89**(8), 2006, p. 082104.
[3] FALCONY C., KIRTLEY J.R., DIMARIA D.J., MA T.P., CHEN T.C., *Electroluminescence emission from indium oxide and indium–tin–oxide*, Journal of Applied Physics **58**(9), 1985, pp. 3556–3558.
[4] GRANQVIST C.G., *Transparent conductive electrodes for electrochromic devices: A review*, Applied Physics A **57**(1), 1993, pp.19–24.
[5] BENDER M., KATSARAKIS N., GAGAOUDAKIS E., HOURDAKIS E., DOULOUFAKIS E., CIMALLA V., KIRIAKIDIS G., *Dependence of the photoreduction and oxidation behavior of indium oxide films on substrate temperature and film thickness*, Journal of Applied Physics **90**(10), 2001, pp. 5382–5387.
[6] CHAO LI, DAIHUA ZHANG, BO LEI, SONG HAN, XIAOLEI LIU, CHONGWU ZHOU, *Surface treatment and doping dependence of In_2O_3 nanowires as ammonia sensors*, Journal of Physical Chemistry B **107**(45), 2003, pp. 12451–12455.
[7] TOMITA T., YAMASHITA K., HAYAFUJI Y., ADACHI H., *The origin of n-type conductivity in undoped In_2O_3*, Applied Physics Letters **87**(5), 2005, p. 051911.
[8] ROSEN J., WARSCHKOW O., *Electronic structure of amorphous indium oxide transparent conductors*, Physical Review B **80**(11), 2009, p. 115215.
[9] ERHART P., KLEIN A., EGDELL R.G., ALBE K., *Band structure of indium oxide: Indirect versus direct band gap*, Physical Review B **75**(15), 2007, p. 153205.
[10] The film was obtained from Applied Film. Hall measurements were done on the BioRad system at NREL.
[11] OHTA H., ORITA M., HIRANO M., TANJI H., KAWAZOE H., HOSONO H., *Highly electrically conductive indium–tin–oxide thin films epitaxially grown on yttria-stabilized zirconia (100) by pulsed-laser deposition*, Applied Physics Letters **76**(19), 2000, pp. 2740–2742.
[12] VAN HEST M.F.A.M., DABNEY M.S., PERKINS J.D., GINLEY D.S., TAYLOR M.P., *Titanium-doped indium oxide: A high-mobility transparent conductor*, Applied Physics Letters **87**(3), 2005, p. 032111.
[13] GUPTA R.K., GHOSH K. MISHRA S.R., KAHOL P.K., *High mobility Ti-doped In_2O_3 transparent conductive thin films*, Materials Letters **62**(6–7), 2008, pp. 1033–1035.
[14] YANG MENG, XI-LIANG YANG, HUA-XIAN CHEN, JIE SHEN, YI-MING JIANG, ZHUANG-JIAN ZHANG, ZHONG-YI HUA, *Molybdenum-doped indium oxide transparent conductive thin films*, Journal of Vacuum Science and Technology A **20**(1), 2002, pp. 288–290.
[15] NEWHOUSE P.F., PARK C.-H., KESZLER D.A., TATE J., NYHOLM P.S., *High electron mobility W-doped In_2O_3 thin films by pulsed laser deposition*, Applied Physics Letters **87**(11), 2005, p. 112108.
[16] KARAZHANOV S.ZH., RAVINDRAN P., VAJEESTON P., ULYASHIN A., FINSTAD T.G., FJELLVÅG H., *Phase stability, electronic structure, and optical properties of indium oxide polytypes*, Physical Review B **76**(7), 2007, p. 075129.
[17] MAREZIO M., *Refinement of the crystal structure of In_2O_3 at two wavelengths*, Acta Crystallographica **20**(6), 1966, pp. 723–728.
[18] YOSHIDA Y., WOOD D.M., GESSERT T.A., COUTTS T.J., *High-mobility, sputtered films of indium oxide doped with molybdenum*, Applied Physics Letters **84**(12), 2004, pp. 2097–2099.
[19] ASHIDA T., MIYAMURA A., OKA N., SATO Y., YAGI T., TAKETOSHI N., BABA T., SHIGESATO Y., *Thermal transport properties of polycrystalline tin-doped indium oxide films*, Journal of Applied Physics **105**(7), 2009, p. 073709.
[20] JCPDS Card No. 06-0416, JCPDS International Center for Diffraction Data, Swarthmore, USA.
[21] CULLITY B.D., *Elements of X-ray Diffraction*, 2nd Ed., Addison Wisely, London, 1978.
[22] PARK C.-Y., YOON S.-G., JO Y.-H., SHIN S.-C., *Room-temperature ferromagnetism observed in Mo-doped indium oxide films*, Applied Physics Letters **95**(12), 2009, p. 122502.
[23] http://www.webelements.com/webelements/elements/text/periodic-table/radii.html.
[24] BURSTEIN E., *Anomalous optical absorption limit in InSb*, Physical Review **93**(3), 1954, pp. 632–633.
[25] MEDVEDEVA J.E., *Magnetically mediated transparent conductors: In_2O_3 doped with Mo*, Physical Review Letters **97**(8), 2006, p. 086401.

[26] HUANG L.M., ÅRHAMMAR C., MOYSÉS ARAÚJO C., SILVEARV F., AHUJA R., *Tuning magnetic properties of In_2O_3 by control of intrinsic defects*, Europhysics Letters **89**(4), 2010, p. 47005.
[27] MRYASOV O.N., FREEMAN A.J., *Electronic band structure of indium tin oxide and criteria for transparent conducting behavior*, Physical Review B **64**(23), 2001, p. 233111.
[28] KANAI Y., *Electrical properties of indium–tin–oxide single crystals*, Japanese Journal of Applied Physics, Part 2: Letters **23**(1),1984, pp. L12–L14.
[29] HWANG J.-H., EDWARDS D.D., KAMMLER D.R., MASON T.O., *Point defects and electrical properties of Sn-doped In-based transparent conducting oxides*, Solid State Ionics **129**(1–4), 2000, pp. 135–144.

Received October 2, 2010
in revised form November 28, 2010